A one-dimensional macrocyclic π-ligand conductor carrying a magnetic center. Structure and electrical, optical and magnetic properties of TPP[Fe(Pc)(CN)₂]₂ {TPP = tetraphenylphosphonium and [Fe(Pc)(CN)₂] = dicyano(phthalocyaninato)iron(III)}

Masaki Matsuda,[a] Toshio Naito,[a] Tamotsu Inabe,*[a] Noriaki Hanasaki,[b] Hiroyuki Tajima,[b] Takeo Otsuka,[c] Kunio Awaga,[c] Bakhyt Narymbetov[d] and Hayao Kobayashi[d]

[a]Division of Chemistry, Graduate School of Science, Hokkaido University, Sapporo 060-0810, Japan. E-mail: inabe@sci.hokudai.ac.jp
[b]Institute for Solid State Physics, The University of Tokyo, Roppongi 7-22-1, Minato-ku, Tokyo, 106-8666, Japan
[c]Department of Basic Science, Graduate School of Arts and Science, The University of Tokyo, Tokyo 153-0041, Japan
[d]Institue for Molecular Science, Myodaiji, Okazaki 444-8585, Japan

A conducting partially oxidized salt of TPP[Fe(Pc)(CN)₂]₂, which contains paramagnetic iron(III), has been obtained by electrocrystallization of TPP[Fe(Pc)(CN)₂]. The crystal is composed of one-dimensional TPP arrays surrounded by slipped-stacked one-dimensional Fe(Pc)(CN)₂ chains. This structure is isomorphous with TPP[Co(Pc)(CN)₂]₂, in which the central metal is non-magnetic cobalt(III). The electrical conductivity at room temperature, $ca.$ $10 \, \Omega^{-1} \, cm^{-1}$, is about one order of magnitude lower than that of the Co analogue. On lowering the temperature, the conductivity shows a much steeper decline compared with the temperature dependence of the conductivity of TPP[Co(Pc)(CN)₂]₂. The band width, estimated from both thermoelectric power measurements (which show apparent metallic behavior at high temperatures) and an extended Hückel calculation, is found to be the same as that obtained for TPP[Co(Pc)(CN)₂]₂. This is consistent with observations from the single-crystal reflectance spectra, in which both partially oxidized salts show almost the same plasma edge. On the other hand, the magnetic susceptibility of TPP[Fe(Pc)(CN)₂]₂ is quite different from that of TPP[Co(Pc)(CN)₂]₂; both of the magnetic moments originated from Fe^{III} and the π-radical seem to be localized in TPP[Fe(Pc)(CN)₂]₂, while the moments originated from the π-radical in TPP[Co(Pc)(CN)₂]₂ are interacting with each other to lead to temperature-independent Pauli-like susceptibility. At low temperatures, a decrease in the susceptibility has been observed, suggesting the existence of antiferromagnetic interactions.

The phthalocyanine (Pc) π-ligand has a relatively small ionization potential, and is used as a component of molecular and polymeric conductors.[1] Typically these consist of one-dimensional face-to-face stacking Pc columns and one-dimensional anion chains, i.e. [M(Pc)$_y$X (M = Ni, Cu, H₂, Pt, etc.; X = I₃, ClO₄, AsF₆, SbF₆, etc.).[2–5] Recently, we have reported another type of one-dimensional conductor based on the axially substituted phthalocyanine anion, [Co^{III}(Pc)(CN)₂]⁻.[6] When the simple salt with TPP (tetraphenylphosphonium) is electrochemically oxidized, a partially oxidized salt, TPP[Co^{III}(Pc)(CN)₂]₂, is obtained. The π–π overlap between the Pc rings is partial due to the existence of the axial CN ligands, yet the Pc units form a one-dimensional chain. Since the effective charge on the Co^{III}(Pc)(CN)₂ unit is −0.5, each Pc π-ligand is oxidized by 0.5 e. The estimated HOMO–HOMO overlap integral in this partially oxidized salt was found to be about half that in the one-dimensional face-to-face stacking Pc column. Nevertheless, the observed conductivity at room temperature is still relatively high; $120 \, \Omega^{-1} \, cm^{-1}$.

One advantage of adopting such macrocyclic π-ligands as a component of molecular conductors is facile replacement of the central metal ion with retention of the crystal structure. Since the ligand-field due to Pc and CN is strong, the octahedral configuration imposes the low-spin state to the central metal ion and d⁶ Co^{III} becomes non-magnetic. If the central metal is replaced by Fe^{III}, the d⁵ configuration results in $S = 1/2$. Thus,

we can introduce a magnetic moment in the center of the π-ligand which forms the path of charge transport. Such conductors containing a local magnetic moment are currently attracting considerable attention. A representative example is provided by the perovskite-type manganese oxides[7] which are known to show colossal magnetoresistance caused by cooperation between the conduction electrons and the magnetic ordering of local spins. In molecular conductors, similar π–d interaction has been noted. For example, the molecular conductor λ-(BETS)₂MX (BETS = bis(ethylenedithio)tetraselenafulvalene, M = Fe$_x$Ga$_{1−x}$, and X = Br$_y$Cl$_{4−y}$) was found to show various anomalies, such as superconductor-to-insulator transition,[8] colossal magnetoresistance,[9] meta-magnetic molecular metal behaviour,[10] and so on, arising from the π–d interaction. In most magnetic molecular conductors, local spins are introduced in a counter ion component which does not participate in charge transport. In the case of conductors based on macrocyclic π-ligands, the introduced magnetic metal ion constitutes the conduction part. This situation is expected to lead a different π–d interaction. Such examples have been reported only for the face-to-face stacked M(Pc)X-type conductors with M = Cu^{II} and Co^{II}.[11,12] In these cases, the existence of a kind of π–d interaction has been suggested, but its nature is not yet clear. Here, we have approached this subject by using axially-substituted phthalocyanines. In this paper, we describe the preparation, structure, and electrical,

optical and magnetic properties of a magnetic one-dimensional conductor, TPP[Fe^{III}(Pc)(CN)$_2$]$_2$, in comparison with the Co^{III} analogue.

Experimental

Materials

In the case of the cobalt analogue, the starting potassium salt, K[Co^{III}(Pc)(CN)$_2$], was readily obtained from Co^{II}(Pc) through air oxidation by refluxing the ethanol suspension with excess KCN.[6] A similar procedure led to K$_2$[Fe^{II}(Pc)(CN)$_2$] in the case of Fe^{II}(Pc). Reaction of Fe^{III}(Pc)Cl with KCN yielded a mixture of K[Fe^{III}(Pc)(CN)$_2$] and K$_2$[Fe^{II}(Pc)(CN)$_2$], which was extremely difficult to purify. Therefore, K$_2$[Fe^{II}(Pc)(CN)$_2$] was used as the starting salt. The cation exchange was carried out by metathesis of K$_2$[Fe^{II}(Pc)(CN)$_2$] (0.95 g) with tetra-phenylphosphonium bromide (1.14 g) in acetonitrile (100 ml). The obtained (TPP)$_2$[Fe^{II}(Pc)(CN)$_2$] was then oxidized to TPP[Fe^{III}(Pc)(CN)$_2$] with a stoichiometric amount of bromine in acetone, followed by recrystallization from acetonitrile. The completeness of the oxidation was confirmed by recording the electronic spectra of an acetonitrile solution of the salt in the visible region.

An electrocrystallization cell equipped with a glass frit between the two compartments was filled with *ca.* 30 ml of an acetonitrile solution of TPP[Fe(Pc)(CN)$_2$] (0.4–0.5 mmol dm^{-3}). A constant current of typically 1 μA was applied between two platinum electrodes immersed in the solution of each compartment for 1–2 weeks at 20 °C. Needle-shaped crystals grew on the anode surface as the current flowed, and were harvested by filtration. The single phase crystalline product, TPP[Fe(Pc)(CN)$_2$]$_2$, was obtained even when the current was varied (1–2 μA).

X-Ray structure analysis

An automated Rigaku AFC-7R diffractometer with graphite-monochromated Mo-Kα radiation was used for data collection with a standard method ($2\theta-\omega$ scan, up to 55° in 2θ), and the crystal data are summarized in Table 1. Three standard reflections, which were monitored every 150 data measurements, showed no significant deviation in intensities. The structure was solved by a direct method (SIR-92),[13] and the hydrogen atoms were placed at their calculated ideal positions. A full-matrix least-squares technique with anisotropic thermal parameters for non-hydrogen atoms and isotropic ones for hydrogen atoms (thermal parameters are 1.2 times those of the attached carbons) was employed for the structure refinement, using the teXsan program package.[14]

CCDC reference number 1145/199. See http://www.rsc.org/suppdata/jm/a9/a909159i/ for crystallographic files in .cif format.

Table 1 Crystal data for TPP[Fe(Pc)(CN)$_2$]$_2$

Chemical formula	C$_{92}$H$_{52}$N$_{20}$PFe$_2$
Molecular weight	1580.22
Crystal system	Tetragonal
Space group	$P4_2/n$
a/Å	21.722(2)
c/Å	7.448(2)
V/Å^3	3514.4(5)
Z	2
μ(Mo-Kα)/cm^{-1}	5.05
Temperature of data collection/K	293
No. of reflections measured	4579
No. of independent reflections observed	3142 [$I > 2\sigma(I)$]
R_{int}	0.0145
R	0.036
Rw	0.038

Measurements

Electrical conductivity was measured in the temperature range 12–300 K. In this range, the resistivity varied widely (10^{-1}–10^9 Ω cm, due to the thin needle shape of the crystals the sample resistance, R, varied between 10^0–10^{12} Ω), and special care was taken over the measurements. In the high temperature region ($R < 10^8$ Ω), the standard four-probe method with contacts by gold paste was applied. In the lower region, at which temperature R exceeds the measureable limit of our four-probe method, the measurement was switched to a two-probe method. The two-probe measurement was also extended into the higher temperature region, where the four-probe method gave reliable values, in order to make sure that the contact resistance was small enough and that its temperature dependence was negligible compared with that of the sample crystal. The reproducibility was also checked using several crystals. The thermoelectric power measurement was carried out using a system similar to that reported by Chaikin and Kwak.[15]

The polarized reflectance spectra of the single crystals of TPP[Co(Pc)(CN)$_2$]$_2$ and TPP[Fe(Pc)(CN)$_2$]$_2$ were measured using an Olympus MMSP microspectrophotometer from 4200 to 25 000 cm^{-1} and with a Jasco FTIR 8900 μ microspectrophotometer from 500 to 4200 cm^{-1}. The crystal face and the crystal axes of the sample were determined by the X-ray diffraction technique.

Magnetic susceptibility measurements for randomly oriented sample crystals were performed using Quantum Design MPMS-5 and -XL SQUID susceptometers. The applied field was 1 T, and the background contribution was measured separately. The diamagnetic core contribution was estimated from the independent susceptibility measurements of TPP·Br, (TPP)$_2$[Fe^{II}(Pc)(CN)$_2$] and TPP[Co^{III}(Pc)(CN)$_2$].
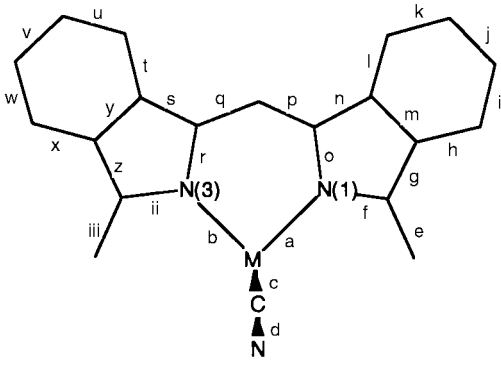
Results and discussion

Molecular and crystal structure of TPP[Fe(Pc)(CN)$_2$]$_2$

Substitution of Co^{III} by Fe^{III} was expected to barely influence the molecular structure, especially since the geometry of the Pc framework is insensitive to the central ion in many cases. The bond lengths derived for the Pc unit are summarized in Table 2 with the corresponding data for TPP[Co(Pc)(CN)$_2$]$_2$.[6] As expected, the bond lengths in the Pc ligand are almost the same for both cases. However, the distance between the metal and the axial CN ligand is slightly longer in Fe^{III}(Pc)(CN)$_2$ than in Co^{III}(Pc)(CN)$_2$, reflecting the slightly larger ionic radius of Fe^{III} compared with Co^{III}. The 1:2 ratio of cation:Pc unit gives an effective charge of −0.5 for one [Fe^{III}(Pc)(CN)$_2$] unit. Therefore, each Pc ring is formally oxidized by 0.5 e from the initial closed-shell Pc^{2-}.

The crystal structure of TPP[Fe^{III}(Pc)(CN)$_2$]$_2$ is shown in Fig. 1. The small difference in the molecular geometry arising from substitution of Co^{III} with Fe^{III} has no effect on the molecular arrangement. The obtained crystal structure is completely isomorphous with TPP[Co(Pc)(CN)$_2$]$_2$.[6] The π–π overlap between the Pc rings is partial due to the existence of the axial CN ligands, yet the Pc units form a one-dimensional chain along the c-axis. The special symmetry of the cation, $\bar{4}$, induces tetragonal arrangement of the one-dimensional Pc chains. The repeat unit of the one-dimensional chain corresponds to the length of the c-axis.

The structure of the one-dimensional chain is shown in Fig. 1(b). The Pc rings, which are translationally related along the c-axis, are stacked with overlaps at two of the four peripheral benzene rings with interplanar distances of 3.47 and 3.40 Å. These values are comparable to those observed for TPP[Co(Pc)(CN)$_2$]$_2$ (3.46 and 3.40 Å).[6] The effectiveness of this stacking mode has been evaluated from an extended Hückel

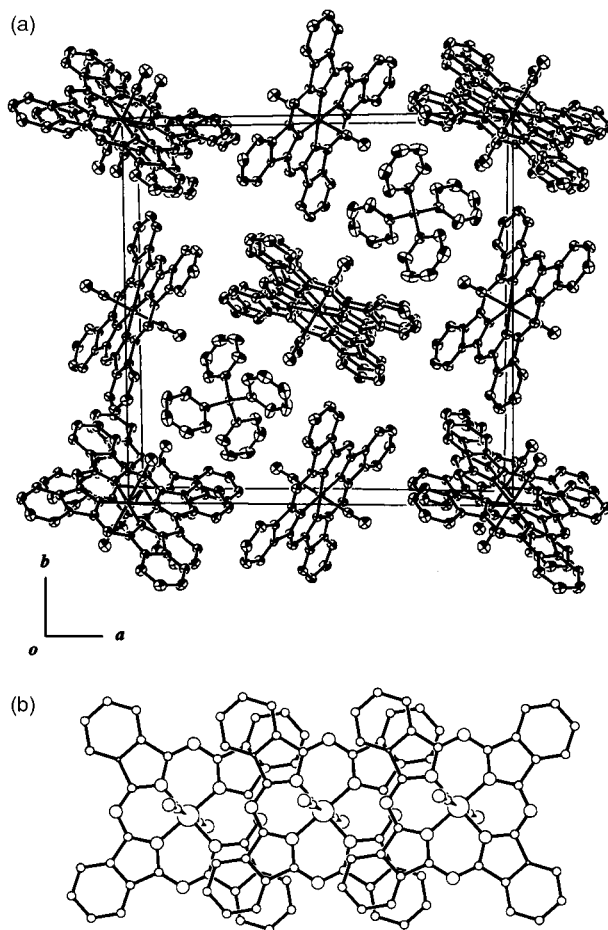**Table 2** Bond lengths (Å) in the M(Pc)(CN)$_2$ unit

Bond	TPP[Co(Pc)(CN)$_2$]$_2$	TPP[Fe(Pc)(CN)$_2$]$_2$
a	1.926(4)	1.942(2)
b	1.943(4)	1.941(2)
c	1.936(5)	1.981(2)
d	1.146(7)	1.142(3)
e	1.324(7)	1.323(2)
f	1.375(7)	1.372(2)
g	1.471(7)	1.462(3)
h	1.390(8)	1.385(3)
i	1.387(8)	1.388(3)
j	1.395(8)	1.390(3)
k	1.392(9)	1.388(3)
l	1.391(7)	1.386(3)
m	1.386(7)	1.391(3)
n	1.450(7)	1.455(3)
o	1.378(6)	1.374(2)
p	1.323(7)	1.323(2)
q	1.325(7)	1.325(3)
r	1.373(6)	1.376(2)
s	1.461(7)	1.456(3)
t	1.394(7)	1.390(3)
u	1.376(8)	1.386(3)
v	1.396(8)	1.388(3)
w	1.392(8)	1.391(3)
x	1.393(8)	1.385(3)
y	1.381(7)	1.388(3)
z	1.463(7)	1.464(3)
ii	1.371(7)	1.370(2)
iii	1.320(7)	1.322(2)

(a)

(b)

Fig. 1 Crystal structure of TPP[Fe^{III}(Pc)(CN)$_2$]$_2$; view along the c-axis (a) and molecular stacking in the Fe(Pc)(CN)$_2$ chain (b).

calculation based on these structural data. The overlap integral between the Pc rings in a chain is calculated to be 8.7×10^{-3} at 293 K, which is almost the same as that of TPP[Co(Pc)(CN)$_2$]$_2$ (8.5×10^{-3} at 296 K).

Charge transport in TPP[Fe(Pc)(CN)$_2$]$_2$

The temperature dependence of the resistivity along the c-axis is shown in Fig. 2, together with that of TPP[Co(Pc)(CN)$_2$]$_2$. The value at room temperature is 1.9×10^{-1} Ω cm, which is nearly one order of magnitude higher than that of TPP[Co(Pc)(CN)$_2$]$_2$ (8.2×10^{-3} Ω cm).[6] The temperature dependence is semiconducting and the apparent activation energy varies with temperature, with a clear inflection point near 35 K. The activation energy of conduction is 0.023 eV around 150 K, 0.016 eV around 55 K, and 0.030 eV below 30 K. This behavior is dramatically different from that of TPP[Co(Pc)(CN)$_2$]$_2$, in which very weak semiconducting behavior with an activation energy of less than 0.01 eV has been observed. The difference in the resistivity becomes very large at lower temperatures (at 14 K, the ratio becomes 10^9).

Fig. 3 shows the temperature dependence of the thermoelectric power. The positive values are consistent with the carrier being a hole generated by oxidation of the Pc π-electrons. In contrast to the conductivity behavior, the thermoelectric power shows clear metallic behavior at high

temperatures. The values and the slope of the linear portion are quite close to those observed for TPP[Co(Pc)(CN)$_2$]$_2$.[6] Assuming a one-dimensional tight-binding band structure, the band width is estimated to be 0.50 eV from the slope above 100 K, which is nearly the same as that estimated for TPP[Co(Pc)(CN)$_2$]$_2$ (0.46 eV).[6] The estimated band width value is also consistent with the calculated overlap integral based on the structural data.

The inconsistency between the thermoelectric power and conductivity, which appears in both the Co and Fe salts, is not totally unreasonable, since the resistance response to the current flow by the external electric field does not necessarily appear in the electromotive force due to the entropy gradient. A typical example is heavily doped polyacetylene films; the thermoelectric power is clearly metallic,[16] while the temperature dependence of the conductivity is thermally activated, even for the highly oriented films.[17] The highly one-dimensional character of the present materals could produce a similar effect. Another important factor is the rather narrow band widths of these materals which will cause a strong electron–electron correlation effect. As a matter of fact, when the effective band width is increased by the chain doubling in [PXX][Co(Pc)(CN)$_2$][18] (PXX = peri-xanthenoxanthene), in which the [Co(Pc)(CN)$_2$]$^{0.5-}$ units form a ladder chain with uniform spacing {and a similar overlap integral value to TPP[Co(Pc)(CN)$_2$]$_2$} along the one-dimensional chain direction, the temperature dependence of the conductivity becomes clearly metallic. These features, the highly one-dimensional character and the narrow band width, may be responsible for the discrepancy between the thermoelectric power and conductivity.

Below 45 K, a steep increase in the thermoelectric power appears. This temperature nearly corresponds to the inflection
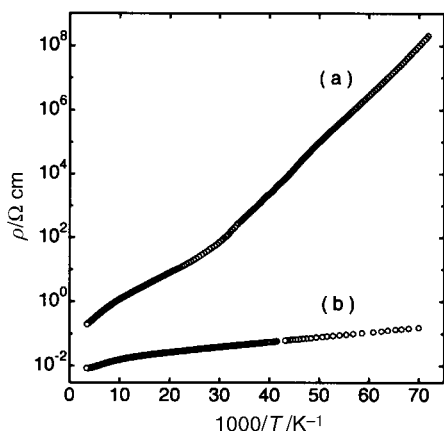
Fig. 2 Temperature dependence of the single-crystal resistivity ($\|c$) of TPP[Fe^{III}(Pc)(CN)$_2$]$_2$ (a) and TPP[Co^{III}(Pc)(CN)$_2$]$_2$ (b).

point observed in the resistivity measurements. This type of change in thermoelectric power is reminiscent of a metal–insulator transition. The possibility of a structural transition was thus examined by a structure analysis at 30 K.[19] The crystal structure at 30 K was found to be practically the same as that obtained at 293 K. This means that any kind of lattice deformation, such as the Peierls distortion, does not occur above 30 K.

Optical spectra of TPP[Co(Pc)(CN)$_2$]$_2$ and TPP[Fe(Pc)(CN)$_2$]$_2$

Fig. 4 shows the reflectance spectra of TPP[Fe^{III}(Pc)(CN)$_2$]$_2$ and TPP[Co^{III}(Pc)(CN)$_2$]$_2$ at room temperature for the polarization parallel and perpendicular to the stacking axis ($E_\|c$ and $E_\|a$), respectively. The $E_\|c$ spectrum exhibits a plasma edge (around 5300 cm^{-1} in the Co^{III} salt; around 5400 cm^{-1} in the Fe^{III} salt) and an outstanding dispersion (peaking at around 8700 cm^{-1} in the Co^{III} salt; around 9000 cm^{-1} in the Fe^{III} salt). The latter dispersion has not been reported in the spectroscopic studies of [M(Pc)]$_y$X.[20]

We analyzed the reflectance spectra using the Lorentz-type complex dielectric function given by;

$$\varepsilon(\omega) = \varepsilon_\infty - \sum_m \frac{\Omega_{pm}^2}{\omega^2 - \Omega_m^2 - i\Gamma_m\omega} \quad (1)$$

and the relation between the reflectance and the complex dielectric function;

$$R(\omega) = \left| \frac{\sqrt{\varepsilon(\omega)} - 1}{\sqrt{\varepsilon(\omega)} + 1} \right|^2 \quad (2)$$

The best fits to the model are shown as a solid line in Fig. 4. The set of parameters which gave the best fits are listed in Table 3. Here we should note that Ω_1 and Ω_{p1} correspond to the gap energy and plasma frequency determined by optical spectro-
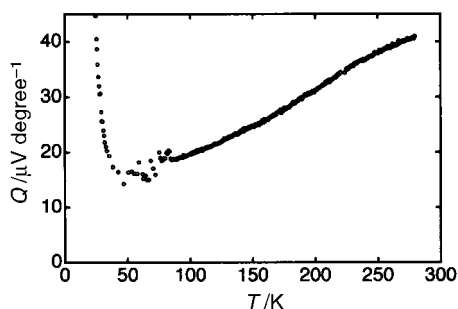

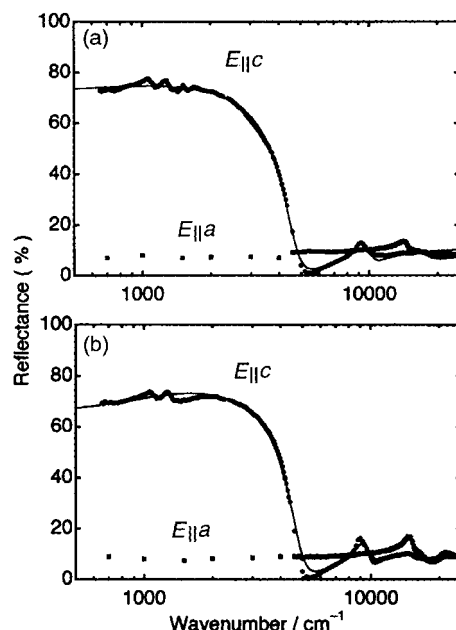Fig. 3 Temperature dependence of the single-crystal thermoelectric power (Q) of TPP[Fe^{III}(Pc)(CN)$_2$]$_2$.

Fig. 4 Single-crystal optical reflectance spectra of TPP[Fe^{III}(Pc)(CN)$_2$]$_2$ (a) and TPP[Co^{III}(Pc)(CN)$_2$]$_2$ (b). The solid lines are the best fit obtained by the parameter set listed in Table 3.

scopy. The gap energy thus determined is much higher than the corresponding energy determined by the transport measurements for the Co^{III} salt[6] and still slightly larger than that for the Fe^{III} salt.

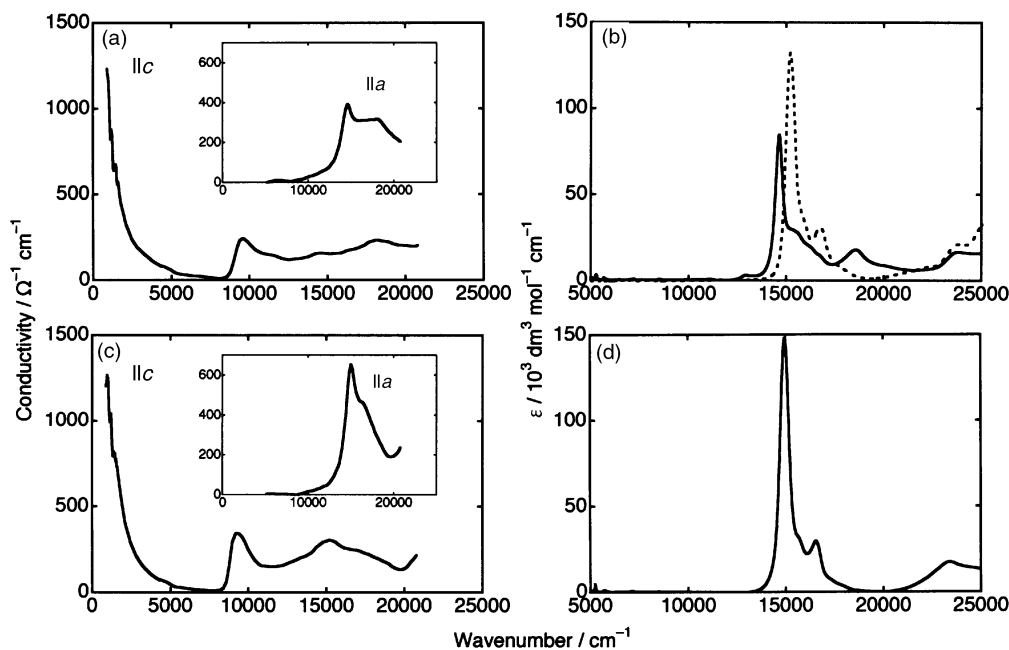According to the 1D tight-binding model, the width of the π-band, $4t$, is given by

$$4t = \frac{\hbar^2 V_c \Omega_{p1}^2}{4e^2 d^2 \sin k_F d} \quad (3)$$

where V_c is the volume fraction per M(Pc)(CN)$_2$ unit and d is the spacing between the M(Pc)(CN)$_2$ units along the 1D axis. The band widths calculated by use of eqn. (3) are also listed in Table 3 and are in good agreement with those estimated from the thermoelectric power.

Fig. 5 shows the conductivity spectra for the polarizations $E_\|a$ and $E_\|c$ obtained through the Kramers–Kronig transformation of the reflectance spectra. The absorption spectra of solutions containing [Fe^{II}(Pc)(CN)$_2$]$^{2-}$, [Fe^{III}(Pc)(CN)$_2$]$^-$ or [Co^{III}(Pc)(CN)$_2$]$^-$ are also illustrated in the figure. For either TPP[Fe(Pc)(CN)$_2$]$_2$ or TPP[Co(Pc)(CN)$_2$]$_2$, the features of the conductivity spectra for both polarizations above 13 000 cm^{-1} are consistent with those of solutions containing the corresponding monovalent anion, {[Fe^{III}(Pc)(CN)$_2$]$^-$ or [Co^{III}(Pc)(CN)$_2$]$^-$}. On the other hand, the peak around 9500 cm^{-1} in the $E_\|c$ conductivity spectra does not appear in

Table 3 Optical and electronic parameters obtained from the reflectance spectra of TPP[Fe(Pc)(CN)$_2$]$_2$ and TPP[Co(Pc)(CN)$_2$]$_2$

|	TPP[Fe(Pc)(CN)$_2$]$_2$	TPP[Co(Pc)(CN)$_2$]$_2$
ε_∞	3.95	3.99
Ω_1/cm^{-1}	789	1090
Ω_{p1}/cm^{-1}	9631	10197
Γ_1/cm^{-1}	1246	1250
Ω_2/cm^{-1}	9967	9468
Ω_{p2}/cm^{-1}	4706	4884
Γ_2/cm^{-1}	1627	1107
Ω_3/cm^{-1}	—	15077
Ω_{p3}/cm^{-1}	—	6627
Γ_3/cm^{-1}	—	3399
d/Å	7.457	7.474
V_c/Å^3	879.87	877.75
$4t$/eV	0.55	0.62

Fig. 5 The conductivity spectra obtained through the Kramers–Kronig transformation of the reflectance spectra of $TPP[Fe^{III}(Pc)(CN)_2]_2$ (a) and the absorption spectra of solutions containing $[Fe^{II}(Pc)(CN)_2]^{2-}$ (broken line) or $[Fe^{III}(Pc)(CN)_2]^{-}$ (solid line) (b). The corresponding spectra of $TPP[Co^{III}(Pc)(CN)_2]_2$ (c) and $[Co^{III}(Pc)(CN)_2]^{-}$ (d).

the $E_{\parallel}a$ conductivity spectra nor in the absorption spectra. Thus we assigned this peak to the charge-transfer excitation, although a corresponding charge-transfer band has not been reported for $[M(Pc)]_yX$. Since the excitation energy of this charge-transfer band exceeds the width of the conduction band, we assigned the transition to the charge-transfer band between different kinds of molecular orbitals. Such charge-transfer excitation has been reported in the conducting salts of $Pd(dmit)_2$.[21]

Magnetic susceptibility of $TPP[Co(Pc)(CN)_2]_2$ and $TPP[Fe(Pc)(CN)_2]_2$

The temperature dependence of the magnetic susceptibility of $TPP[Co^{III}(Pc)(CN)_2]_2$ and $TPP[Fe^{III}(Pc)(CN)_2]_2$ is shown in Fig. 6. The data are corrected for the background and the core diamagnetic contribution. For $TPP[Co^{III}(Pc)(CN)_2]_2$, the small paramagnetic susceptibility is almost temperature-independent, suggesting Pauli-like susceptibility. The value $(7.7 \times 10^{-4}$ emu mol$^{-1})$ is, however, much larger than that expected for a simple one-dimensional metal with a band width estimated from the thermoelectric power and optical measurements. This enhancement may suggest that the electron–electron correlation effect in this system is relatively large, as proposed earlier.

On the other hand, the paramagnetic susceptibility of $TPP[Fe(Pc)(CN)_2]_2$ shows a high temperature dependence. In this salt, there are two kinds of spins; π-radical-centered spin $(S=1/2)$ and Fe^{III}-centered spin $(S=1/2)$. The concentration of the latter is twice that of the former, and one formula unit, $TPP[Fe^{III}(Pc)(CN)_2]_2$, contains $3 \times S = 1/2$ spins. At high temperatures, the susceptibility nearly correlates to inverse temperature, suggesting Curie-like paramagnetism. If we assume $g = 2$ for all the spins and the absence of magnetic exchange interactions between them, the $\chi_p T$ value [Fig. 6(c)] would be 1.125 emu mol^{-1} K. The observed value at high temperature is much higher than for the above assumption. However, in preliminary measurements of the susceptibility using orientated crystals it was found that the anisotropy is extremely large. Some preferential orientation (especially for the thin needle crystals) may be one possible origin of this large $\chi_p T$ value. Another noticeable feature is that the π-centered
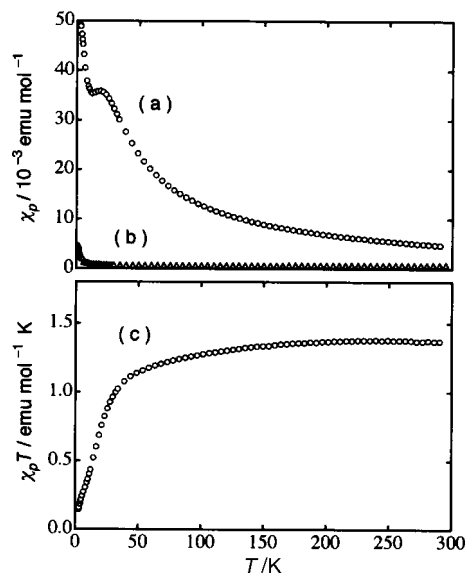
Fig. 6 Temperature dependence of the magnetic susceptibility (χ_p) of randomly orientated polycrystalline samples; χ_p for $TPP[Fe^{III}(Pc)(CN)_2]_2$ (a) and $TPP[Co^{III}(Pc)(CN)_2]_2$ (b), and $\chi_p T$ for $TPP[Fe^{III}(Pc)(CN)_2]_2$ (c).

spin behaves as a localized spin. Though the conductivity of $TPP[Fe^{III}(Pc)(CN)_2]_2$ is lower than that of $TPP[Co^{III}(Pc)(CN)_2]_2$, it is still much higher than that expected for a localized electron system, at least at high temperatures.

In the low-temperature region, an anomaly at around 20 K is apparent. This drop in susceptibility suggests the appearance of some antiferromagnetic interaction, and it was found that this anomaly is also anisotropic. From the $\chi_p T$ value at the lowest temperature, both π-radical and Fe^{III} spins seem to be involved in this susceptibility drop. Since the shortest $Fe^{III} \cdots Fe^{III}$ distance is more than 7 Å, the magnetic exchange interaction must occur through the overlapped π-ligands. In addition, there are π-radical spins in the overlapped π-ligands. The total picture of the magnetic interactions seems to be very complicated and cannot be explained solely on the basis of the present results. This complicated situation (spins are not

independent), however, suggests that this material is a good candidate for a novel π–d coupled system. In fact, we have recently found that TPP[Fe^{III}(Pc)(CN)$_2$]$_2$ shows giant negative magnetoresistance[22] below the inflection point in the temperature dependence of the resistivity. This fact indicates that the conduction electrons are sensitive to the local magnetic moments of Fe^{III}.

In conclusion, we have succeeded in introducing the magnetic Fe^{III} ion into a one-dimensional conductor based on axially-substituted phthalocyanine. The resultant crystals of TPP[Fe^{III}(Pc)(CN)$_2$]$_2$ have a completely isomorphous structure with the non-magnetic Co^{III} analogue. The π–π overlap integral estimated from the Hückel calculation is the same as that of the Co^{III} analogue, and is consistent with the temperature dependence of the thermoelectric power above 100 K and the reflectance spectra at room temperature. On the other hand, marked differences between the Fe^{III} and Co^{III} salts lie in the electrical conductivity and magnetic susceptibility. Since no structural transition has been observed down to 30 K, the differences are believed to arise from the magnetic moment of Fe^{III}. At the present stage, there are many unknown factors in this system concerning the nature of the magnetic coupling between the localized spins and between the conduction electrons and the localized spins. Detailed studies on the magnetic properties using oriented single crystals and EPR measurements at low temperature (no signal was detected down to 77 K) are now in progress to elucidate the details of the magnetic interaction. Also, the Fe^{III} and Co^{III} alloy system is expected to provide valuable information about the π–d interaction, and crystal growth and characterization is now under way.

References

1   T. J. Marks, *Angew. Chem., Int. Ed. Engl.*, 1990, **29**, 857.
2   C. S. Schramm, R. P. Scaringe, D. R. Stojakovic, B. M. Hoffman, J. A. Ibers and T. J. Marks, *J. Am. Chem. Soc.*, 1980, **102**, 6702; J. Martinsen, S. M. Palmer, J. Tanaka, R. Greene and B. M. Hoffman, *Phys. Rev. B*, 1984, **30**, 6269.
3   T. Inabe, T. J. Marks, R. L. Burton, J. W. Lyding, W. J. McCarthy, C. R. Kannewurf, G. M. Reisner and F. H. Herbstein, *Solid State Commun.*, 1985, **54**, 501.
4   T. Inabe, S. Nakamura, W. Liang, T. J. Marks, R. L. Burton, C. R. Kannewurf and K. Imaeda, *J. Am. Chem. Soc.*, 1985, **107**, 7224.
5   K. Yakushi, M. Sakuda, H. Kuroda, A. Kawamoto and J. Tanaka, *Chem. Lett.*, 1986, 1161.
6   H. Hasegawa, T. Naito, T. Inabe, T. Akutagawa and T. Nakamura, *J. Mater. Chem.*, 1998, **8**, 1567.
7   H. Y. Hwang, S.-W. Cheong, P. G. Radaelli, M. Marezio and B. Batlogg, *Phys. Rev. Lett.*, 1995, **75**, 914; B. Raveau, A. Maignan and B. Caignaert, *J. Solid State Chem.*, 1995, **117**, 424; Y. Tomioka, A. Akimitsu, Y. Morimoto, H. Kuwahara and Y. Tokura, *Phys. Rev. Lett.*, 1995, **74**, 5108; H. Kuwahara, Y. Tomioka, A. Akimitsu, Y. Morimoto and Y. Tokura, *Science*, 1995, **270**, 961; H. Kuwahara, Y. Tomioka, Y. Morimoto, A. Akimitsu, M. Kasai, R. Kumai and Y. Tokura, *Science*, 1996, **272**, 80.
8   H. Kobayashi, A. Sato, E. Arai, H. Akutsu, A. Kobayashi and P. Cassoux, *J. Am. Chem. Soc.*, 1997, **119**, 12 392.
9   H. Akutu, K. Kato, E. Arai, H. Kobayashi, A. Kobayashi, M. Tokumoto, L. Brossard and P. Cassoux, *Solid State Commun.*, 1998, **105**, 485.
10 L. Brossard, R. Clerac, C. Coulon, M. Tokumoto, T. Ziman, D. K. Petrov, V. N. Laukin, M. J. Naughton, A. Audouard, F. Goze, A. Kobayashi, H. Kobayashi and P. Cassoux, *Eur. Phys. J.*, 1998, **B1**, 439.
11 M. Y. Ogawa, J. Martinsen, S. M. Palmer, J. L. Stanton, J. Tanaka, R. L. Greene, B. M. Hoffman and J. A. Ibers, *J. Am. Chem. Soc.*, 1987, **109**, 1115.
12 H. Yamakado, T. Ida, A. Ugawa, K. Yakushi, K. Awaga, Y. Maruyama, K. Imaeda and H. Inokuchi, *Synth. Met.*, 1994, **62**, 169; T. Hiejima and K. Yakushi, *J. Chem. Phys.*, 1995, **103**, 3950.
13 A. Altomare, M. C. Burla, M. Camalli, M. Cascarano, C. Giacovazzo, A. Guagliardi and G. Polidori, *J. Appl. Crystallogr.*, 1994, **27**, 435.
14 teXsan, Crystal Structure Analysis Package, Molecular Structure Corporation, 3200 Research Forest Drive, The Woodlands, TX 77381, 1985 and 1992.
15 P. M. Chaikin and J. F. Kwak, *Rev. Sci. Instrum.*, 1975, **46**, 429.
16 E. B. Park, J. S. Yoo, J. Y. Park, Y. W. Park, K. Akagi and H. Shirakawa, *Synth. Met.*, 1995, **69**, 61; Y. W. Park, C. O. Yoon, C. H. Lee, H. Shirakawa, Y. Suezaki and K. Akagi, *Synth. Met.*, 1989, **28**, D27.
17 N. Basescu, Z.-X. Liu, D. Moses, A. J. Heeger, H. Naarmann and N. Theophilou, *Nature*, 1987, **327**, 403; Th. Schimmel, G. Denninger, W. Riess, J. Voit, M. Schwoerer, W. Schoepe and H. Naarmann, *Synth. Met.*, 1989, **28**, D11.
18 S. Takano, T. Naito and T. Inabe, *Chem. Lett.*, 1998, 1249.
19 Low temperature (30 K) structure analysis was performed by using an area detector system (Mo-Kα radiation) equipped with a liquid helium cooling device. The crystal data are as follows; space group $P4_2/n$, $a = 21.407(7)$, $b = 7.386(5)$ Å, $V = 3385(2)$ Å^3, $Z = 2$, and the final $R = 0.058$ ($Rw = 0.076$) for 3025 observed reflections [$I > 2\sigma(I)$].
20 K. Yakushi, H. Yamakado, M. Yoshitake, N. Kosugi, H. Kuroda, A. Kawamoto, J. Tanaka, T. Sugano and M. Kinoshita, *Synth. Met.*, 1989, **29**, F95.
21 H. Tajima, T. Naito, M. Tamura, A. Kobayashi, H. Kuroda, R. Kato, H. Kobayashi, R. A. Clark and A. E. Underhill, *Solid State Commun.*, 1991, **79**, 337.
22 N. Hanasaki, H. Tajima, M. Matsuda, T. Naito and T. Inabe, *Phys. Rev. B*, submitted.

Paper a909159i